Cent. Eur. J. Phys. • 9(5) • 2011 • 1209-1220
DOI: 10.2478/s11534-011-0046-z

VERSITA

Central European Journal of **Physics**

Nondipole parameters of TDCS for electron impact ionization and drag current

Research Article

Arkadiy S. Baltenkov[1]*, Steven T. Manson[2], Alfred Z. Msezane[3],

1 *Arifov Institute of Electronics, 100125, Tashkent, Uzbekistan*

2 *Department of Physics and Astronomy, Georgia State University, Atlanta, Georgia 30303, USA*

3 *Center for Theoretical Studies of Physical Systems, Clark Atlanta University, Atlanta, Georgia 30314, USA*

Received 27 January 2011; accepted 23 April 2011

Abstract: A comprehensive study is undertaken of angular distributions of electron knock-out from atomic targets by fast electrons with a small transfer of momentum. The general expressions for the parameters of the triple differential cross-section of impact ionization in the optical limit are derived. The calculated parameters are compared with those of the angular distribution of electrons ejected from an atom in the process of photoionization. In these processes, when the multipole transitions are involved, the one-to-one correspondence between the photoionization and impact ionization parameters disappears. The nondipole transitions lead to the backward/forward asymmetry of the angular distribution of ejected electrons that is absent in the dipole approximation for ionization by both fast electrons and photons. Using the He atom as an example, the character of the asymmetry for these two processes is qualitatively different and the backward/forward asymmetry results in macroscopic directed motion of secondary electrons accompanying the passing of a fast electron beam through gas or plasma. The general formulas for this drag current are derived and applied to gaseous He.

PACS (2008): 34.80.Dp, 34.90.+q

Keywords: Impact ionization • triple differential cross-section • back/forward asymmetry • non-dipole parameters • drag current

1. Introduction

Atomic ionization by fast electrons is of importance in a variety of areas, including physics. The study of inelastic collisions stems from the ever-increasing need of plasma and radiation physics, astrophysics, atmospheric physics, *etc.* [1–10]. For a number of cases, the energy and angular distributions of the ejected electrons are very important to understand – for example, the track structure in radiation physics [2, 9]. The basic quantity that describes the angular distribution of knock-out electrons and the energy lost by the fast incident electron is the triple

*E-mail: arkbalt@mail.ru

differential cross-section (TDCS), the differential in solid angle of the scattering fast particle, the solid angle of the ionized secondary electron, and the energy lost by the scattered projectile. Integration of TDCS over the solid angle of the scattered particle yields the double differential cross-section (DDCS), which gives the energy and angular distribution of ionized electrons. Integration of the DDCS over the solid angle of the ionized electrons gives the single differential cross-section (SDCS), the energy distribution of secondary electrons. Each integration eliminates many details of the impact ionization process. Therefore, the complete information about this process is contained in the TDCS. For this reason its study is of great interest.

It is known that the main role in impact ionization is played by the processes with a small amount of fast electron momentum transferred to target atoms. Therefore, among the numerous studies of the TDCS (both experimental and theoretical [11–19]), an important place is occupied by investigations focusing specifically on studying of the TDCS in the optical limit (see, for example [20] and references therein), when the cross-section for a small amount of transferred momentum $\mathbf{q}$ can be represented as a power series in momentum. In the limit $q \to 0$ the TDCS is well described by the dipole approximation [21–23]. In this approach, the amplitudes for dipole transitions of atomic electrons to the continuum define the angular distribution of ejected electrons. Therefore, the angular distribution of ejected electrons for small q is similar to the differential cross-section for dipole photoionization of atoms, that is, both the angular distributions are described by a linear combination of the Legendre polynomials of zero and second orders. The difference is that the argument of these polynomials in the electron scattering process is the cosine of the angle between the momentum transfer $\mathbf{q}$ and the momentum of the ejected electron $\mathbf{k}$; in the case of photoionization, between the photon polarization vector e and $\mathbf{k}$. The coefficients of the Legendre polynomials – the parameters of the differential cross-section – define the shape of the angular distribution of ejected electrons. These parameters depend on dipole matrix elements and phase shifts of the continuum wave functions. Of interest is, first, to compare these parameters for both processes in the dipole approximation and, second, to analyze whether there is a one-to-one correspondence between the parameters of both angular distributions beyond the dipole approximation.

The main corrections to the differential cross-sections for these processes in the optical limit result from interference of the amplitudes for dipole and quadrupole transitions of atomic electrons [24–28]. In the case of atomic ionization these studies now constitute rapidly developing investigations (see [31] and references therein). A comparative study of similar parameters in the differential cross-sections of impact ionization of atoms significantly extends the available ideas about the dynamics of both optically allowed and forbidden transitions of atomic electrons. In addition, the existence of $E1$-$E2$ nondipole contributions to photoionization leads to backward/forward asymmetry in the angular distribution of ejected electrons. For this reason the passing of ionizing radiation through a gas target is accompanied by directed photoelectron motion known as a drag current [24, 25, 30]. A similar effect should be expected while passing a beam of fast charged particles through gas or plasma.

In this context it is reasonable to study, in the optical limit, the first non-dipole corrections in the TDCS and to discuss the problem of electron dragging in gas under the action of a fast electron beam, not only as a new physical phenomenon but also as a possible method to investigate one of the nondipole terms in the differential cross-section of charged particle impact ionization. The present paper is devoted to an investigation of these problems.

The plan of the paper is as follows. In Sec. 2, within the framework of the Plane Wave Born Approximation (PWBA), the general formulas for the parameters of angular distribution of knock-out electrons relative to the transferred momentum are derived. These general formulas are used in Sec. 3 to derive the TDCS parameters in the optical limit. Further, by using the electron impact ionization of the He atom as an example, a comparison of the angular distributions of ejected electrons calculated in the dipole approximation is performed, taking into account the nondipole corrections; the backward/forward asymmetry of the angular distributions due to the nondipole transitions in both processes is analyzed. In Sec. 4 the formulas for the parameters of the electron angular distribution relative to the incident projectile direction are obtained. They are used in Sec. 5 to derive the general formulas for the drag current in atomic gases and to calculate the drag current in gaseous helium. Sec. 6 gives the summary conclusions. The Appendix of the paper is devoted to comparing the general formulas for the dipole parameters for charged particle impact- and photo-ionization of p- and d-atomic subshells.

2. TDCS within the PWBA

We consider a fast electron with initial momentum $\mathbf{p}_1$ and kinetic energy $T = p_1^2/2$ ionizing a stationary atomic nl_0-state (atomic units are used throughout the paper). Further, let the momentum of the scattered fast electron be $\mathbf{p}_2$, so that the momentum transferred to the atom is

$\mathbf{q} = \mathbf{p}_2 - \mathbf{p}_1$. For this process the TDCS, the differential in ejected electron energy ε [or, equivalently, energy lost by the impinging fast electron $\varepsilon + I$ (where I is the ionization energy of the atomic electron)], and the differential in both the ejected electron direction and in the scattered fast-electron direction is given within PWBA by [21–23].

$$\frac{d^3\sigma}{d\varepsilon d\Omega_{p_2} d\Omega_k} = \frac{kp_2}{2\pi^3 q^4 p_1}\left|\int \psi_f^* \sum_j e^{-i\mathbf{q}\cdot\mathbf{r}_j}\psi_0 d\tau\right|^2 \quad (1)$$

Here $d\Omega_k$ and $d\Omega_{p_2}$ are the differential solid angles in the directions of the ejected electron and the scattered fast electron, respectively. If we express Ψ_0 and Ψ_f as asymmetric products of single-particle functions, Eq. (1) reduces to

$$\frac{d^3\sigma}{d\varepsilon d\Omega_{p_2} d\Omega_k} = \frac{N_{nl_0} kp_2}{2\pi^3 q^4 p_1}\left|\langle \mathbf{k}|e^{-i\mathbf{q}\cdot\mathbf{r}}|0\rangle\right|^2 \quad (2)$$

where N_{nl_0} is the number of electrons in the initial nl_0 atomic subshell. The single-particle atomic wave function for the initial and final atomic states have the following forms

$$|0\rangle = R_{nl_0}(r)Y_{l_0m_0}(\mathbf{r});$$
$$|\mathbf{k}\rangle = \Psi_k^-(\mathbf{r}) = 4\pi\sum_{\lambda,\mu} i^\lambda e^{-i\delta_\lambda} R_{k\lambda}(r)Y_{\lambda\mu}(\mathbf{k})Y_{\lambda\mu}^*(\mathbf{r}) \quad (3)$$

where R_{nl_0} and $R_{k\lambda}(r)$ are the radial parts of the electron wave functions in the initial and final states. The wave function of the knocked-out electron $|\mathbf{k}\rangle$ asymptotically is a plane wave $\exp(i\mathbf{k}\cdot\mathbf{r})$ propagating in the direction $\mathbf{k}$ plus incoming spherical waves; λ and $\mathbf{k}$ are the electron orbital moment and momentum, respectively; $\delta_\lambda(k)$ are the associated phase shifts.

For fixed values of the initial and final momenta of the fast electron, $\mathbf{p}_1$ and $\mathbf{p}_2$, the momentum transfer vector $\mathbf{q}$ is fixed in space. In this case the angular distribution of ejected electrons depends only on the angle between the vectors $\mathbf{q}$ and $\mathbf{k}$ and has the form [31, 32]

$$\frac{d^3\sigma}{d\varepsilon d\Omega_{p_2} d\Omega_k} = \frac{2N_{nl_0} kp_2}{\pi^2 q^4 p_1} \times \sum_{l,\lambda}\sum_{l',\lambda'}\sum_L (2l+1)(2\lambda+1)(2l'+1)(2\lambda'+1)(-1)_{l_0+L}\cos(\Delta_{l\lambda}-\Delta_{l'\lambda'})Q_{l_0 l}^{\lambda} Q_{l_0 l'}^{\lambda'}$$
$$\times \begin{pmatrix} l_0 & l & \lambda \\ 0 & 0 & 0 \end{pmatrix}\begin{pmatrix} l_0 & l' & \lambda' \\ 0 & 0 & 0 \end{pmatrix}\begin{pmatrix} \lambda & \lambda' & L \\ 0 & 0 & 0 \end{pmatrix}\begin{pmatrix} l & l' & L \\ 0 & 0 & 0 \end{pmatrix}\begin{Bmatrix} \lambda & \lambda' & L \\ l' & l & l_0 \end{Bmatrix}(2L+1)P_L(\cos\upsilon) \quad (4)$$

Here the $P_L(\cos\upsilon)$ are the Legendre polynomials; υ is the angle between the vectors $\mathbf{k}$ and $\mathbf{q}$; $\Delta_{l\lambda} = \delta_\lambda - \pi(l+\lambda)/2$. The radial matrix elements in Eq. (4) are defined by the integrals

$$Q_{l_0 l}^{\lambda}(q) = \int R_{nl_0}(r) j_l(qr) R_{k\lambda}(r) r^2 dr \quad (5)$$

Here $j_l(qr)$ are the spherical Bessel functions [33].

Integration of Eq. (4) over $d\Omega_k$ gives $4\pi\delta_{L0}$, which eliminates all terms in this equation except the term with $L = 0$. The differential cross-section relative to the vector $\mathbf{q}$ with the fixed vector $\mathbf{p}_2$ and the differential in energy loss and scattering angle has the form

$$\frac{d^2\sigma}{d\varepsilon d\Omega_{p_2}} = \frac{8N_{nl_0} kp_2}{\pi q^4 p_1}\sum_{l,\lambda}(2l+1)(2\lambda+1)\begin{pmatrix} l_0 & l & \lambda \\ 0 & 0 & 0 \end{pmatrix}^2 \left|Q_{l_0 l}^{\lambda}\right|^2 \quad (6)$$

To compare the TDCS with the photoelectron angular distribution, Eq. (4) is rewritten as

$$\frac{d^3\delta}{d\varepsilon d\Omega_{p_2} d\Omega_k} = \frac{1}{4\pi}\frac{d^2\sigma}{d\varepsilon d\Omega_{p_2}}\sum_{L=0} B_L P_L(\cos\upsilon) \quad (7)$$

The desired expression for the coefficients B_L, defining a shape of the angular distribution of secondary electron momentum $\mathbf{k}$ relative to the vector $\mathbf{q}$ (that in this experiment is fixed in space), is the following fourfold sum

$$B_L = \frac{1}{S_0^{l_0}} \sum_{l,\lambda} \sum_{l',\lambda'} (2l+1)(2\lambda+1)(2l'+1)(2\lambda'+1) \cos(\Delta_{l\lambda} - \Delta_{l'\lambda'}) Q^{\lambda}_{l_0 l}(q) Q^{\lambda'}_{l_0 l'}(q) \times \begin{Bmatrix} l_0 & l & \lambda \\ 0 & 0 & 0 \end{Bmatrix} \begin{Bmatrix} l_0 & l' & \lambda' \\ 0 & 0 & 0 \end{Bmatrix} \begin{Bmatrix} l & l' & L \\ 0 & 0 & 0 \end{Bmatrix} \begin{Bmatrix} \lambda & \lambda' & L \\ 0 & 0 & 0 \end{Bmatrix} \begin{Bmatrix} \lambda & \lambda' & L \\ l' & l & l_0 \end{Bmatrix} (-1)^{l_0+L}(2L+1) \quad (8)$$

where $S_0^{l_0}$ in the denominator is the following double sum

$$S_0^{l_0} = \sum_{l,\lambda} (2l+1)(2\lambda+1) \left| Q^{\lambda}_{l_0 l} \right|^2 \begin{Bmatrix} l_0 & l & \lambda \\ 0 & 0 & 0 \end{Bmatrix}^2 \quad (9)$$

Eqs. (7)–(9) describe in general the TDCS for atoms by charged-particle impact ionization, taking into account all orders of the transferred momentum $\mathbf{q}$.

3. Optical limit for TDCS

The TDCS dependence [Eq. (4)] on transferred momentum is totally concentrated in the matrix elements of Eq. (5). Let a be the radius of electron localization in the initial atomic state. Then the region in the vicinity of a near the atomic nucleus is the primary contributor to the matrix elements in Eq. (5). In this case a criterion of passing to the optical limit $q \to 0$ is satisfying the inequality $qa \ll 1$. In this limit the Bessel function in the matrix elements of Eq. (5) is represented as a decreasing series in powers of (qr) [33]. Keeping in this series the first principal terms, we obtain for $q \to 0$ the following expressions for the matrix elements of Eq. (5)

$$\begin{aligned} Q^{\lambda}_{l_0 0}\big|_{q\to 0} &= -\frac{q^2}{6} \int R_{nl_0}(r) r^2 R_{k\lambda}(r) r^2 dr \\ &= -\frac{q^2}{6} \langle k\lambda | r^2 | n, l_0 \rangle, \quad \text{for } l = 0, \\ Q^{\lambda}_{l_0 l}\big|_{q\to 0} &= \frac{q^l}{(2l+1)!!} \int R_{nl_0}(r) r^l R_{k\lambda}(r) r^2 dr \\ &= \frac{q^l}{(2l+1)!!} \langle k\lambda | r^l | n, l_0 \rangle, \quad \text{for } l \neq 0. \end{aligned} \quad (10)$$

According to Eq. (10), for small transferred momenta, an order-of-magnitude approximation for the matrix element products in the sum in Eq. (8) is $l + l'$. The main contribution to the sum in Eq. (8) in the optical limit is made by the terms with minimal power $\sim q^2$, that is, the dipole matrix elements with $l = l' = 1$. The terms of the next order $\sim q^3$ are the products of the dipole and quadrupole matrix elements. The nondipole corrections to the atomic photoionization cross-section are defined by the products of the same matrix elements $E1$-$E2$. Having in mind a further comparison of the coefficients B_L with the parameters of the photoelectron angular distribution, we restrict them to terms of order $\sim q^3$ in the fourfold sum in Eq. (8). These terms in the sum in Eq. (8) correspond to the orbital momenta l and $l' = 0$, 1, and 2.

The general formulas Eqs. (8) and (9) for arbitrary initial atomic states are rather cumbersome. Therefore, we restrict ourselves here to consideration of the impact ionization parameters B_L for the s-atomic states. The p- and d- initial atomic states are considered in the Appendix. The fourfold sum in Eq. (8) for $l_0 = 0$ is transformed to the twofold one. Substituting $L = 0$, 1, 2, and 3 in it and keeping the terms of order $\sim q^3$, we obtain for the first four parameters of the TDCS the following expressions

$$\begin{aligned} B_0 &= 1, \\ B_1 &= \frac{q}{5\langle k, p|r|n, s\rangle} [5\langle k, s|r^2|n, s\rangle \cos(\delta_0 - \delta_1) \\ &\quad - 4\langle k, d|r^2|n, s\rangle \cos(\delta_1 - \delta_2)], \\ B_2 &= 2, \\ B_3 &= \frac{6}{5} q \frac{\langle k, d|r^2|n, s\rangle}{\langle k, p|r|n, s\rangle} \cos(\delta_1 - \delta_2). \end{aligned} \quad (11)$$

Comparing (11) with the formulas in [20], it should be noted that the transferred momentum in [20] is defined as a difference of the vectors $\mathbf{p}_1 - \mathbf{p}_2$. This vector differs by a sign from the vector $\mathbf{q}$ used in the present paper. Therefore, to compare the formulas, the expressions for the parameters of the TDCS in [20] should be multiplied by $(-1)^L$. Let us compare now the coefficients of Eq. (11) with the parameters defining the photoelectron angular distribution.

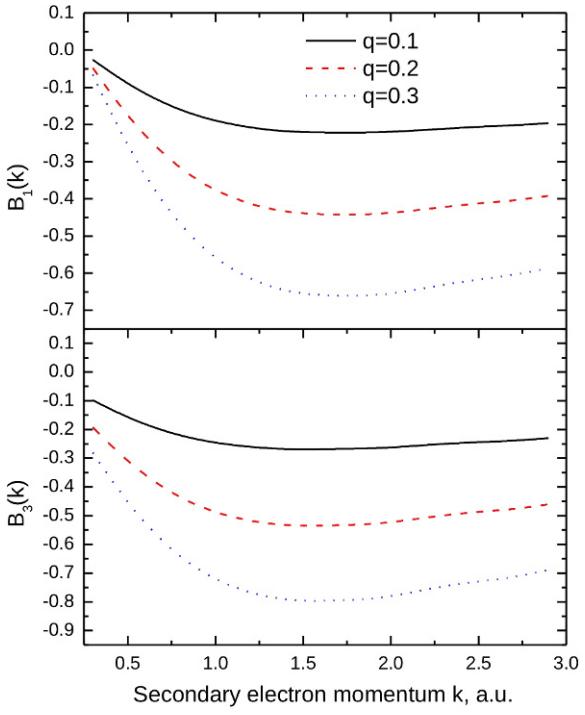

Figure 1. Non-dipole asymmetry parameters B_1 and B_3 as the functions of k for fixed transferred momentum q.

In the dipole approximation, the differential cross-section for photoionization by polarized photons is a linear combination of the two Legendre polynomials of zero and second orders [34]

$$\frac{d\sigma(\omega)}{d\Omega_k} = \frac{\sigma(\omega)}{4\pi}[P_0(\cos\upsilon) + \beta P_2(\cos\upsilon)]. \qquad (12)$$

The angle υ here is the angle between the photon polarization vector **e** and the photoelectron momentum vector **k**; $\sigma(\omega)$ is the total photoionization cross-section. For photoionization of the atomic s-subshell, the coefficients of $P_0(\cos\upsilon)$ and $P_2(\cos\upsilon)$ in the angular distribution in Eq. (12) are equal to $B_0 = 1$ and $B_2 = \beta = 2$, respectively; they exactly coincide with Eq. (11). As shown in the Appendix, the dipole parameters of the TDCS in the optical limit and the parameters of the photoionization differential cross-section in Eq. (12) also coincide in the case of charged-particle impact ionization of the p- and d-atomic subshells. Thus, in the dipole approximation there is one-to-one correspondence between the photoionization and impact ionization parameters. This correspondence has been used experimentally to create a "poor man's synchrotron," a technique that employs electron impact ionization to study photoionization [35].

The situation with the terms of the next order in q is different. For Eq. (11) it is evident that the parameters of the angular distributions B_1 and B_3 cannot coincide with the $E1$-$E2$ corrections in the photoelectron angular distribution. The coincidence is impossible, for example, because the TDCS parameters Eq. (11) are defined also by the amplitude of the monopole transition of an electron from s-atomic state to s-continuum state. These electron transitions are strictly forbidden by the selection rules in the case of photoionization.

The reason for the disappearance of the coincidence between the parameters of the angular distributions is that the interaction with photons is defined by the mutual orientation of three vectors: photon polarization **e**, photon momentum κ, and photoelectron momentum **k**. However, in the electron impact ionization the amplitude, Eq. (2), is a function of only two vectors, **q** and **k**. In other words, for electron impact ionization, within the framework of the PWBA, the momentum transfer **q** is an axis of symmetry for all multipoles, while in photoionization the photon polarization **e** is only an axis of symmetry at the dipole level.

In the process of atom ionization by nonpolarized radiation we deal with one vector only – the vector of photon momentum κ. The photoelectron angular distribution in this case has the form of a linear combination of the Legendre polynomials of the cosine of the angle between the vectors κ and **k** [24, 25], that is, the differential cross-section depends on the mutual disposition of two vectors, as for impact ionization. However, in this case as well, because of the presence of a monopole amplitude, the parameters B_L do not coincide with the photoionization ones. This discrepancy is due principally to the different form of the operators of photon and fast charged particle interaction with atomic electrons.

To illustrate the different roles of the nondipole transitions under electron impact ionization and photoionization, we consider the ionization of the He atom in the ground 1s-state and compare the angular distribution resulting from Eq. (7) with that of the dipole approximation. In the latter case the exponent in the matrix element in Eq. (2) is replaced by the first non-vanishing (in the optical limit) term that is equal to $(-i\mathbf{q}\cdot\mathbf{r})$. The He 1$s$-wave function is localized, that is, maximized at a radius of the order of the Bohr radius. Therefore, we selected for calculation the values $q = 0.1$, 0.2, and 0.3, which correspond to the optical limit in the TDCS. The atomic wave functions in the matrix elements of Eq. (5) were calculated in the Hartree-Fock approximation with previously published codes [36]. The calculated values of these parameters are presented in Fig. 1. These parameters for calculated energies corresponding to the knock-out electrons ε are negative and reach the maximum absolute values for $\varepsilon \sim I_{1s}$, where I_{1s} is the ionization potential of the 1s level of the

He atom. Normalized to unity at an angle $\upsilon = 0$, the TDCS in Eq. (7) for $q = 0.1$ and $k = 1.5$, that is, with the maximum values of the parameters B_1 and B_3, are given in Fig. 2. In this figure the curves for the TDCS both in the dipole approximation and taking into account the first nondipole corrections in Eq. (11) are given in the coordinate system with the vector **q** as a polar axis. In spite of the smallness of the transferred momentum the nondipole corrections are very significant. They result from secondary electrons ejected with very high probability in the direction opposite to the vector $\mathbf{q} = \mathbf{p}_2 - \mathbf{p}_1$, that is, along the momentum vector of the primary fast electrons $\mathbf{p}_1$.

The normalized TDCSs for $q = 0.1$ and $k = 10$ are presented in Fig. 3. For comparison the angular distributions of photoelectrons emitted from the s-atomic states, which are calculated with nondipole corrections, are also included. For the calculation of this cross-section the photon energy ω was set, as it must be, equal to the transferred energy ΔE in the electron impact process. For the calculation of these angular distributions, we chose a very high value of the kinetic energy of the ejected electron, on the atomic scale, so that a shift of the maximum in the photoelectron angular distribution could be seen in the figure. This shift is defined by the ratio k/c where c is the speed of light. Since the non-dipole parameters rapidly decrease with the growth in energy of the ejected electrons, the non-dipole asymmetry in the TDCS is not so pronounced compared to the case of charged particle impact ionization when electrons are ejected with energy $\varepsilon \sim I_{1s}$ (Fig. 2). However, even for these energies it is still quite visible.

The vector **q** is an axis of cylindrical symmetry for the angular distributions of secondary electrons under impact ionization within the PWBA. The curves in Figs. 2 and 3 depict this angular distribution for a fixed azimuth angle φ of electron ejection in the coordinate system with the center at the target-atom nucleus. For comparison with photoionization, a polar axis of this system coincides with the photon polarization vector **e**, and the photon wave vector κ is along the x-axis, located in the plane of the figure. In the dipole approximation the electron- and photon-generated angular distributions coincide (dashed line in both cases), and they have the shape of two lobes symmetrical with respect to both the polar axis **q**(**e**) and the axis κ. When the nondipole transitions are included, the shape of each of these angular distributions changes, but in very different ways. In the case of electron impact ionization, the angular distribution symmetry relative to the polar axis remains unchanged, but the lobe in the lower half-plane becomes larger than the upper one. The ejected electrons are emitted symmetrically about **q**, but the cross-

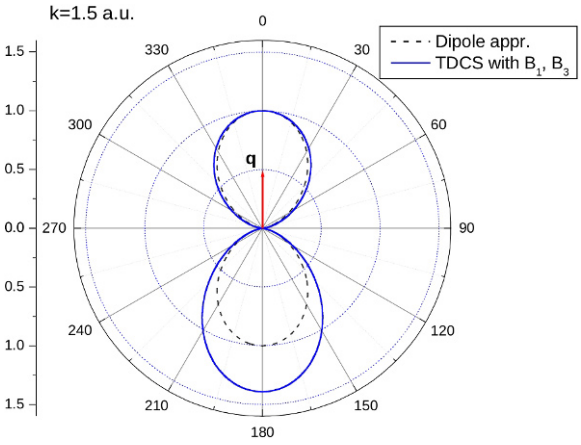

Figure 2. Scaled TDCS as a function of angle between the vectors **q** and **k** for electrons ejected from He, normalized to unity in the forward direction for $q = 0.1$ and $k = 1.5$. The dashed line is the result of the dipole approximation. The incident fast electrons move in this figure from the upper semi-plane to the lower one.

section for ejection in the direction of $+\mathbf{q}$ is smaller than the cross-section for electron emission in the $-\mathbf{q}$ direction. In contrast, for photoionization, the upper and lower lobes of the angular distribution are the same but their maxima deviate from the direction of the polarization vector **e** and shift either towards or away from the photon momentum vector κ.

Thus, the non-dipole corrections, even for small transferred momenta, distort the angular distribution of ejected electrons compared with the dipole picture (Figs. 2 and 3). If, in the processes of charged particle impact ionization

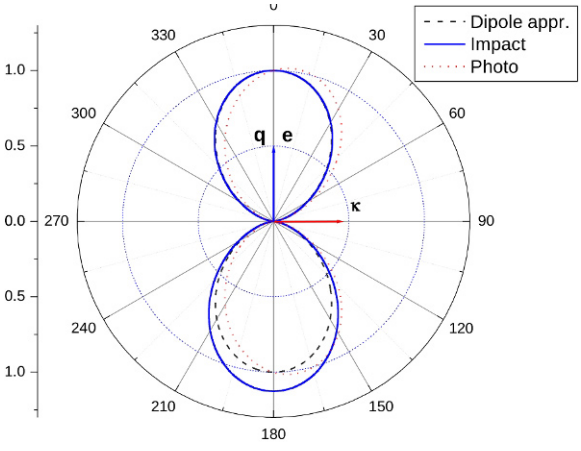

Figure 3. Normalized to unity in the forward direction, TDCS for electrons ejected from He for $q = 0.1$ and $k = 10$. The dashed line is the result of the dipole approximation. The red line is the photoionization cross-section.

and photoionization, not only the dipole transitions are involved but also nondipole ones, the character of the asymmetry of photoionization and charged particle impact ionization spectra is essentially different (Fig. 3), and the one-to-one correspondence between the angular distribution parameters disappears.

4. Double differential cross-section

To obtain the double differential cross-section (DDCS), that is, the energy and angular distribution of secondary electrons relative to the vector $\mathbf{p}_1$, the TDCS in Eq. (4) must be integrated over directions of the vector $\mathbf{p}_2$:

$$\frac{d^2\sigma}{d\varepsilon d\Omega_k} = \int \frac{d^3\sigma}{d\varepsilon d\Omega_{p_2} d\Omega_k} d\Omega_{p_2} \tag{13}$$

This integration can be performed by applying the addition theorem for spherical harmonics [22]. Integration over solid angle $d\Omega_{p_2}$ is transformed into integration over the transferred momentum $\mathbf{q}$ [21–23] and, as a result, we obtain the following expression [31, 32] for the angular distribution of ejected electrons relative to the incident projectile direction $\mathbf{p}_1$:

$$\begin{aligned}\frac{d^2\sigma}{d\varepsilon d\Omega_k} &= \frac{4N_{nl_0}k}{\pi p_1^2}\sum_{l,\lambda}\sum_{l',\lambda'}\sum_{L}(2l+1)(2\lambda+1)(2l'+1)(2\lambda'+1)(-1)^{l_0+L}\cos(\Delta_{l\lambda}-\Delta_{l'\lambda'}) \\ &\times\int_{q_{min}}^{q_{max}} P_L(\cos\upsilon_{qp_1})Q^{\lambda}_{l_0 l}(q)Q^{\lambda'}_{l_0 l'}(q)\frac{dq}{q^3} \\ &\times\begin{Bmatrix} l_0 & l & \lambda \\ 0 & 0 & 0\end{Bmatrix}\begin{Bmatrix} l_0 & l' & \lambda' \\ 0 & 0 & 0\end{Bmatrix}\begin{Bmatrix} \lambda & \lambda' & L \\ 0 & 0 & 0\end{Bmatrix}\begin{Bmatrix} l & l' & L \\ 0 & 0 & 0\end{Bmatrix}\begin{Bmatrix} \lambda & \lambda' & L \\ l & l' & l_0\end{Bmatrix}(2L+1)P_L(\cos\Theta)\end{aligned} \tag{14}$$

Here Θ is the angle between the vectors $\mathbf{p}_1$ and $\mathbf{k}$; $\cos\upsilon_{qp_1} = -(2\Delta E + q^2)/(2qp_1)$ is the cosine of the angle between the vectors $\mathbf{q}$ and $\mathbf{p}_1$. Integration of the DDCS in Eq. (14) over $d\Omega_k$ gives $4\pi\delta_{L0}$, which eliminates all the terms in this equation except the term with $L = 0$. The double differential cross-section for the scattering of the fast charged particle, differential in energy loss and scattering angle, has the form

$$\frac{d^2\sigma}{d\varepsilon d d\Omega_k} = \frac{1}{4\pi}\frac{d\sigma}{d\varepsilon}\sum_{L=0}\overline{B}_L P_L(\cos\Theta), \tag{15}$$

where for the single differential cross-section (SDCS) we have the following formula

$$\frac{d\sigma}{d\varepsilon} = \frac{16N_{nl_0}k}{p_1^2}\sum_{l,\lambda}(2l+1)(2\lambda+1)\begin{Bmatrix} l_0 & l & \lambda \\ 0 & 0 & 0\end{Bmatrix}^2\int_{q_{min}}^{q_{max}}\left|Q^{\lambda}_{l_0 l}(q)\right|^2\frac{dq}{q^3}. \tag{16}$$

The parameters $\overline{B}_L$ in the DDCS of Eq. (15) are defined, as before, by the formulas Eqs. (8) and (9), in which, however, the products of the matrix elements and their squares are replaced by the following integrals

$$\begin{aligned} Q^{\lambda}_{l_0 l}Q^{\lambda'}_{l_0 l'} &\to \int_{q_{min}}^{q_{max}} P_L(\cos\upsilon_{qp_1})Q^{\lambda}_{l_0 l}(q)Q^{\lambda'}_{l_0 l'}(q)\frac{dq}{q^3}, \\ \left|Q^{\lambda}_{l_0 l}\right|^2 &\to \int_{q_{min}}^{q_{max}}\left|Q^{\lambda}_{l_0 l}(q)\right|^2\frac{dq}{q^3}. \end{aligned} \tag{17}$$

The integration limits in these integrals are defined by the energy ΔE transferred during the collisions and have the form

$$q_{max} = p_1 + p_2 = p_1 + \sqrt{p_1^2 - 2\Delta E},$$
$$q_{min} = p_1 - p_2 = p_1 - \sqrt{p_1^2 - 2\Delta E}. \qquad (18)$$

It is evident that the DDCS parameters have nothing to do with either the dipole or $E1$-$E2$ parameters of photoionization, because the integrals of Eq. (16), representing a convolution of the matrix elements and the Legendre polynomials, cannot be transformed into simple products of the matrix elements, as is the case for the parameters of the differential photoionization cross-section [24–28, 34, 36]. In principle, information about the non-dipole parameters B_1 ($\overline{B}_1$) and B_3 ($\overline{B}_3$) can be obtained by measuring the TDCS in Eq. (7) or DDCS in Eq. (15) at the angle $\upsilon = \Theta = \upsilon_m$ [29]. For this so-called magic angle the Legendre polynomial $P_2(\cos\upsilon_m) = 0$, and these differential cross-sections become functions of the non-dipole parameters of lower order in the transferred momentum. It is, however, possible, in principle, to measure one of the DDCS parameters, namely $\overline{B}_1$, in a new type of experiment – by studying microscopic currents accompanying transmission of a fast electron beam through gas or plasma media. We will consider this phenomenon in the next section.

5. Drag current

The backward/forward asymmetry (Figs. 2 and 3) in the differential cross-section for atomic ionization by electron impact can result in the directed motion of electrons through gas or plasma, that is, the electron impact ionization can result in macroscopic drag currents in these media. These currents were discussed in connection with the $E1$-$E2$ corrections in the photoelectron angular distribution and lead to the backward/forward asymmetry in the differential photoionization cross-section [24, 25, 30]. These drag currents were first described for photoionization by Grinberg and Makovsky [38]. They analyzed the role of the photon momentum in the photoionization of shallow impurity centers in semiconductors. They showed that the quadrupole bound-free transitions result in macroscopic drag currents in the direction of the photon momentum. Other mechanisms of electron or hole dragging were considered in [39]. The drag effects in semiconductors were found and studied experimentally [40–42]. Similar effects in atomic gases and plasmas were predicted and described in [24, 25, 30, 43]. The experimental study of drag-effects in gaseous media was hindered by the absence of intense ultraviolet radiation sources capable of ionizing the outer atomic shells in a single-photon process. Recently, however, the first experimental confirmation of drag currents in atomic and molecular gases was reported [44]. The drag currents due to the passing of high-energy beams of heavy charged particles through atomic gases were considered in [45].

Following the methodology of [30], we can obtain formulas for the drag current in an atomic gas target resulting from the ionization by a fast electron beam. We start with the general formula for the drag current appearing under atomic photoionization [30]

$$\mathbf{j}(\omega) = -\mathbf{W}_p \frac{1}{\sigma_{el}(k)} \int \frac{d\sigma_p(k)}{d\Omega_k} \cos\upsilon d\Omega_k, \qquad (19)$$

where $\mathbf{W}_p$ is the photon flux density; $\sigma_{el}(k)$ is the cross-section for elastic scattering of photoelectrons by gas atoms, which define their relaxation time in gas; $d\sigma_p(k)/d\Omega_k$ is the differential cross-section of atomic photoionization; and υ is the angle between the momentum vectors of the photoelectron $\mathbf{k}$ and the photon κ.

For the given case the photon flux density $\mathbf{W}_p$ in Eq. (19) must be replaced by the flux in the beam of the fast electrons $\mathbf{W}$ [$\mathrm{cm}^{-2}\mathrm{s}^{-1}$]. The density of the electric current created by these electrons is in the usual units $\mathbf{j}_0 = -|e|\mathbf{W}$ (e is the electron charge). Following standard procedure, we consider the directed motion of positive charges as constituting the current. Further, in the photoionization process all photoelectrons ejected in the gas have the same energy $\varepsilon = \omega - I$. In the case of electron-impact ionization we deal with the energy spectrum of ejected electrons. Thus, the generalization of Eq. (19) for the case of electron-impact-induced drag currents requires the replacement of the photoionization cross-section with the DDCS from Eq. (15), along with the integration of the projection of $\mathbf{k}$ onto the vector $\mathbf{p}_1$ and integration over the spectrum of ejected electrons. As a result, the drag current $\mathbf{j}$ due to the passing of a beam of fast electrons through an atomic gas is given by

$$\mathbf{j} = \mathbf{j}_0 \int \frac{d^2\sigma}{d\varepsilon d\Omega} \frac{\cos\Theta}{\sigma_{el}(\varepsilon)} d\Omega d\varepsilon.$$

Substituting into Eq. (5) the DDCS from Eq. (15), we obtain for the ratio of the electric currents the following expression

$$\frac{j}{j_0} = \frac{1}{3} \int \frac{d\sigma}{d\varepsilon} \frac{\overline{B}_1}{\sigma_{el}(\varepsilon)} d\varepsilon. \qquad (20)$$

Thus, the directed macroscopic motion of electrons in gas or plasma, initiated by a beam of fast electrons, is defined by only the parameter $\overline{B}_1$ of the DDCS of Eq. (15). For

further consideration of drag currents in gaseous He, we obtain the general expression for the drag current due to electron-impact ionization of s-electrons of atomic gas target.

In the integrals of Eq. (17), defining a convolution of the matrix elements, the main contribution results from the range of transferred momenta q in the vicinity of the lower limit of integration $q \sim q_{min} \approx \Delta E/p_1$. Taking this into account, we represent the nondipole parameter $\overline{B}_1$ by the following expression

$$\overline{B}_1 = \frac{\overline{S}_1 \Delta E}{5p_1 \langle k,1|r|n,0\rangle}, \qquad (21)$$

where the function $\overline{S}_1$ has the form

$$\begin{aligned} \overline{S}_1(\varepsilon) \;=\; & 4\langle k,1|r|n,0\rangle\langle k,2|r^2|n,0\rangle \cos(\delta_2-\delta_1) \\ & -5\langle k,1|r|n,0\rangle\langle k,0|r^2|n,0\rangle \cos(\delta_1-\delta_0). \end{aligned} \qquad (22)$$

Here we use the notation for matrix elements from Eq. (10). For integration of the SDCS of Eq. (16) over the momentum transfer q, we take into account that for small q the integral over dq diverges logarithmically, while within the range of large q the integrand rapidly decreases, owing to the presence of an oscillating function in the matrix elements. Thus, the main role in the integral over dq is played by the range of small q. Therefore, we can restrict the integration from a minimum value $q_{min} \approx \Delta E/p_1$ to some value $\beta \sim 1$ [22]. As a result, we obtain the desired expression for the drag current in PWBA

$$\frac{j}{j_0} = \frac{8N_{n0}}{45T^{3/2}} \int \frac{\overline{S}_1(\varepsilon)}{\sigma_{el}(\varepsilon)} \sqrt{\varepsilon}\Delta E \ln\left[\beta \frac{p_1}{\Delta E}\right] d\varepsilon. \qquad (23)$$

As in the case of the drag current resulting from photoionization, the electron-impact-ionization-induced drag current, Eq. (23), is a function of a combination of the matrix elements and the corresponding phases. The difference is that in the photoionization case, the effect depends on the products of dipole and quadrupole matrix elements, while in the charged particle case, a combination of dipole-monopole and dipole-quadrupole matrix elements Eq. (23) determines the effect. The calculated results for the ratio of the currents $j(T)/j_0$ in gaseous helium as a function of kinetic energy T are presented in Fig. 4. For the calculation, the experimental elastic scattering cross-sections $\sigma_{el}(\varepsilon)$ [46] were used. The density of the drag current rapidly decreases with the growth in energy of the fast electrons T, which is connected with the rapid decrease in the total cross-section for impact

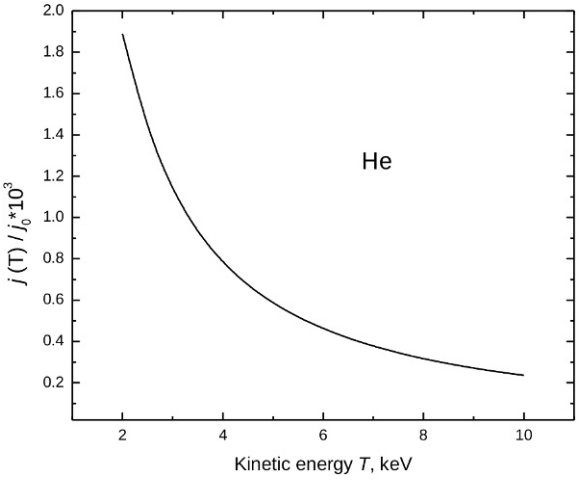

Figure 4. Ratio of drag current to incident electron current $j(T)/j_0$ in gaseous He as a function of kinetic energy T of fast incident electrons

ionization of the atom. The ratio of currents for energies under consideration is ~0.1%. Note that huge values of the drag currents are generated under natural conditions, namely in lightning strikes. It is known that the electric field necessary to initiate such an electric discharge is ~1 MV/m. To maintain the discharge, an electric field of ~0.1–0.2 MV/m [47] is sufficient. In the first stage of the process, in the region where the electric field reaches its critical value, the electron impact ionization starts with the free electrons always available in the air. Owing to the electric field, these electrons acquire significant speeds and undergo ionizing collisions with atmospheric atoms and molecules. Thus, the electron avalanches – streamers – are the conducting channels that, in combination, provide the onset of a bright thermo-ionized channel with high conductivity. The current in this channel ranges from tens to hundreds of thousands of Amperes. The channel length of ground lightning is 1–10 km, and the diameter is several centimeters. Under these conditions the drag current density can reach enormous values of thousands of A/cm^2.

6. Summary and conclusions

We have presented expressions for the TDCS for atoms due to charged particle impact ionization in the optical limit as a series in powers of the transferred momentum. It has been shown that the principal terms of this series are defined by the amplitudes of dipole and quadrupole electron transitions from the bound atomic state to the continuum. The explicit expressions for the first four pa-

rameters of the angular distribution B_L have been obtained for the s-, p- and d-atomic subshells. The calculated parameters are compared with those of the angular distribution of electrons ejected from an atom in the photoionization process. It has been shown that in the PWBA the one-to-one correspondence between the photoionization and charged particle impact ionization parameters remains valid only in the dipole approximation. This correspondence disappears when the transitions of other multiplicity (in particular, quadrupole ones) are involved in the process. Nondipole corrections to the angular distribution of ejected electrons, resulting from electron-impact ionization, proved to be significant even for collisions with small momentum transfer to the target. The nondipole contributions in the TDCS, as in the case of atomic photoionization, result in backward/forward asymmetry, but the character of the asymmetry for these two processes is qualitatively different. Finally, it has been shown that the backward/forward asymmetry in the DDCS leads to preferential motion (along the vector $\mathbf{p}_1$) of secondary electrons in gas targets bombarded by fast electron beams, that is, to the appearance of macroscopic drag currents in gas media. The effect of this dragging under electron impact ionization, under certain conditions, can result in significant values of the drag current, which is important in a number of areas, including atmospheric physics, plasma physics, and space and astrophysics.

Note that for higher photon energies for photoionization, and for higher energy transfer in the charged-particle impact ionization case, still higher multipoles will become important. However, even if the same multipoles are important in the two cases, these multipoles will manifest themselves in different ways in the two cases, owing to the different symmetries of the two processes. In addition, our conclusions would not be altered at all qualitatively by the use of wave functions other than Hartree–Fock in the calculations; nevertheless, they might be changed quantitatively somewhat, but it is not expected that the changes would be very significant.

Acknowledgments

This work was supported by DoE, Division of Chemical Sciences, Office of Basic Energy Sciences, Office of Energy Research, NASA, NSF, CAU CFNM funded by NSF and Uzbek Foundation Award ΦA-Φ2-Φ100.

Appendix A

1. Case of p-atomic states

Substituting in Eq. (9) $l_0 = 1$, and after some angular momentum algebra manipulation, we find for B_L the following expressions:

$$
\begin{aligned}
B_0 &= 1,\\
B_1 &= \frac{9q}{25[\langle k,s|r|n,p\rangle^2 + 2\langle k,d|r|n,p\rangle^2]}[-5\langle k,p|r^2|n,p\rangle\langle k,s|r|n,p\rangle\cos(\delta_1-\delta_0)\\
&\quad + 6\langle k,p|r^2|n,p\rangle\langle k,d|r|n,p\rangle\cos(\delta_1-\delta_2) - 4\langle k,f|r^2|n,p\rangle\langle k,d|r|n,p\rangle\cos(\delta_3-\delta_2)],\\
B_2 &= \frac{2\langle k,d|r|n,p\rangle}{[\langle k,s|r|n,p\rangle^2 + 2\langle k,d|r|n,p\rangle^2]}[\langle k,d|r|n,p\rangle - 2\langle k,s|r|n,p\rangle\cos(\delta_0-\delta_2)],\\
B_3 &= \frac{6q}{25[\langle k,s|r|n,p\rangle^2 + 2\langle k,d|r|n,p\rangle^2]}[5\langle k,f|r^2|n,p\rangle\langle k,s|r|n,p\rangle\cos(\delta_3-\delta_0)\\
&\quad + 6\langle k,p|r^2|n,p\rangle\langle k,d|r|n,p\rangle\cos(\delta_1-\delta_2) - 4\langle k,f|r^2|n,p\rangle\langle k,d|r|n,p\rangle\cos(\delta_3-\delta_2)]. \qquad \text{(A1)}
\end{aligned}
$$

2. Case of *d*-atomic states

For $l_0 = 2$ the parameters B_L are defined by the following expressions

$$
\begin{aligned}
B_0 &= 1,\\
B_1 &= \frac{2q}{35[2\langle k,p|r|n,d\rangle^2 + 3\langle k,f|r|n,d\rangle^2]}[-84\langle k,d|r^2|n,d\rangle\langle k,p|r|n,d\rangle\cos(\delta_2-\delta_1)\\
&\quad + 111\langle k,d|r^2|n,d\rangle\langle k,f|r|n,d\rangle\cos(\delta_2-\delta_3) + 14\langle k,s|r^2|n,d\rangle\langle k,p|r|n,d\rangle\cos(\delta_0-\delta_1)\\
&\quad - 36\langle k,g|r^2n,d\rangle\langle k,f|r|n,d\rangle\cos(\delta_4-\delta_3)],\\
B_2 &= \frac{2}{5[2\langle k,p|r|n,d\rangle^2 + 2\langle k,f|r|n,d\rangle^2]}[6\langle k,f|r|n,d\rangle^2 + \langle k,p|r|n,d\rangle^2 - 18\langle k,f|r|n,d\rangle\langle k,p|r|n,d\rangle\cos(\delta_1-\delta_3)],\\
B_3 &= \frac{6q}{35[2\langle k,p|r|n,d\rangle^2 + 3\langle k,f|r|n,d\rangle^2]}[12\langle k,g|r^2|n,d\rangle\langle k,p|r|n,d\rangle\cos(\delta_4-\delta_1)\\
&\quad - 2\langle k,d|r^2|n,d\rangle\langle k,p|r|n,d\rangle\cos(\delta_2-\delta_1) - 7\langle k,s|r^2|n,d\rangle\langle k,f|r|n,d\rangle\cos(\delta_0-\delta_3)\\
&\quad + 8\langle k,d|r^2|n,d\rangle\langle k,f|r|n,d\rangle\cos(\delta_2-\delta_3) - 6\langle k,g|r^2|n,d\rangle\langle k,f|r|n,d\rangle\cos(\delta_4-\delta_3)]. \qquad \text{(A2)}
\end{aligned}
$$

The dipole asymmetry parameter in the differential cross-section for photoionization, given in Eq. (12) as $\beta(\omega) = B_2$, is defined by the following expression [34]

$$
\beta(\omega) = \frac{l_0(l_0-1)D_{l_0-1}^2 + (l_0+1)(l_0+2)D_{l_0+1}^2 - 6l_0(l_0+1)D_{l_0-1}D_{l_0+1}\cos(\delta_{l_0-1}-\delta_{l_0+1})}{(2l_0+1)[l_0D_{l_0-1}^2 + (l_0+1)D_{l_0+1}^2]}, \qquad \text{(A3)}
$$

where the dipole matrix elements are defined by the integrals

$$
D_{l_0\pm1} = \int R_{nl_0}(r)rR_{kl_0\pm1}(r)r^2dr = \langle k, l_0\pm1|r|n,l_0\rangle. \qquad \text{(A4)}
$$

Sequentially substituting in (A3) $l_0 = 0$, 1, and 2, and taking into account Eq. (10), we obtain for the parameter $\beta(\omega)$ the formulas coinciding with those for the coefficients B_2. Thus, in the dipole approximation there is a one-to-one correspondence between the photoionization and charged particle impact ionization parameters for atomic states *p*-, *d*-, etc.

References

[1] H.S.W. Massey, E.W. McDaniel, B. Bederson (Eds). Applied Atomic Collision Physics (Academic Press, New York, 1983)

[2] Inokuti, In: H.S.W. Massey, E.W. McDaniel, B. Bederson (Eds) Applied Atomic Collision Physics (Academic Press, New York, 1983) 179

[3] T.R. Kallman, P. Palmeri, Rev. Mod. Phys. 79, 79 (2007)

[4] A. Dalgarno, S. Lepp, In: G.W.F. Drake (Ed.) Atomic, Molecular, & Optical Physics Handbook (American Institute of Physics, Woodbury, NY, 1996) 919

[5] J.L. Fox, In: G.W.F. Drake (Ed.) Atomic, Molecular, & Optical Physics Handbook (American Institute of Physics, Woodbury, NY, 1996) 940

[6] J. Weisheit, In: G.W.F. Drake (Ed.) Atomic, Molecular, & Optical Physics Handbook (American Institute of Physics, Woodbury, NY, 1996) 978
[7] A. Garscadden, In: G.W.F. Drake (Ed.) Atomic, Molecular, & Optical Physics Handbook (American Institute of Physics, Woodbury, NY, 1996) 986
[8] E.T. Jensen, In: G.W.F. Drake (Ed.) Atomic, Molecular, & Optical Physics Handbook (American Institute of Physics, Woodbury, NY, 1996) 1007
[9] M. Inokuti, In: G.W.F. Drake (Ed.) Atomic, Molecular, & Optical Physics Handbook (American Institute of Physics, Woodbury, NY, 1996) 1045
[10] N.J. Mason, In: C.T. Whelan, N.J. Mason (Eds) Electron Scattering From Atoms, Molecules, Nuclei and Bulk Matter (Kluwer Academic/Plenum Publishers, New York, 2005) 179
[11] D.H. Madison, R.V. Calhoun, W.N. Shelton, Phys. Rev. A 16, 552 (1977)
[12] B. Brauner, J.S. Briggs, H. Klar, J.T. Broad, T. Rösel, K. Jung, H. Ehrhardt, J. Phys. B 24, 657 (1991)
[13] C. Dupre, A. Lahmam-Bennani, A. Duguet, Meas. Sci. Technol. 2, 327 (1991)
[14] A.S. Kheifets, J. Phys. B 26, 2053 (1993)
[15] S. Jones, D.H. adison, J. Phys. B 27, 1423 (1994)
[16] A. Lahmam-Bennani, J. Electron. Spectrosc. Relat. Phenom. 123, 365 (2002)
[17] M.A. Haynes, B. Lohmann, A. Prideaux, D.H. Madison; J. Phys. B 36, 811 (2003)
[18] F. Catoire, E.M. Staicu Casagrande, M. Nekkab, C. DalCappello, K. Bartschat, A. Lahmam-Bennani, J. Phys. B 39, 2827 (2006)
[19] A. Naja et al., J. Phys. B 41, 085205 (2008)
[20] M. Žitnik, L. Avaldi, R. Camilloni, G. Stefani, J. Phys. B 26, L851 (1993)
[21] H. Bethe, In: H. Geiger, K. Sheel (Eds) Handbuch der Physik (Springer, Berlin, 1933)
[22] L.D. Landau, E.M. Lifshitz, Quantum Mechanics, Non-Relativistic Theory (Pergamon Press, Oxford, 1965)
[23] M. Inokuti, Rev. Mod. Phys. 43, 297 (1971)
[24] M.Ya. Amusia, A.S. Baltenkov, A.A. Grinberg, S.G. Shapiro, Sov. Phys. J. Exp. Theor. Phys+. 41, 14 (1975)
[25] M.Ya. Amusia, P.U. Arifov, A.S. Baltenkov, A.A. Grinberg, S.G. Shapiro, Phys. Lett. A 47, 66 (1975)
[26] J.W. Cooper, Phys. Rev. A 42, 6942 (1990)
[27] J.W. Cooper, Phys. Rev. A 45, 3362 (1992)
[28] J.W. Cooper, Phys. Rev. A 47, 1841 (1993)
[29] B. Krässig et al., Phys. Rev. Lett. 75, 4736 (1995)
[30] M.Ya. Amusia, A.S. Baltenkov, L.V. Chernysheva, Z. Felfli, A.Z. Msezane, J. Nordgren, Phys. Rev. A 63, 052512 (2001)
[31] S.T. Manson, L.H. Toburen, D.H. Madison, N. Stolterfoht, Phys. Rev. A 12, 60 (1975)
[32] D.H. Madison, S.T. Manson, Phys. Rev. A 20, 825 (1979)
[33] M. Abramowitz, I.A. Stegun (Eds) Handbook of Mathematical Functions (Dover, New York, 1965)
[34] J. Cooper, R.N. Zare, J. Chem. Phys. 48, 942 (1968)
[35] A.P. Hitchcock, J. Electron Spectrosc. Relat. Phenom. 112, 9 (2000) and references therein
[36] M.Ya. Amusia, L.V. Chernysheva, In: A Handbook of the Atom Programs (Institute of Physics Publishing, Bristol, 1997)
[37] M.Ya. Amusia, A.S. Baltenkov, L.V. Chernysheva, Z. Felfli, A.Z. Msezane, Phys. Rev. A 63, 052506 (2001)
[38] A.A. Grinberg, L.L. Makovsky, Sov. Phys. Semicond. 4, 981 (1970)
[39] A.S. Baltenkov, N.A. Brynskikh, V.B. Gilerson, N.I. Kramer, Sov. Phys. Semicond. 4, 1589 (1970)
[40] A.A. Grinberg, Sov. Phys. J. Exp. Theor. Phys+. 31, 531 (1970)
[41] A.M. Danishevsky, A.A. Kastalsky, S.M. Rivkin, I.D. Yaroshecky, Sov. Phys. J. Exp. Theor Phys+. 31, 292 (1970)
[42] A.F. Gibson, M.E. Kimmit, A.C. Welker, Appl. Phys. Lett. 17, 75 (1970)
[43] M.Ya. Amusia, A.S. Baltenkov, Sov. Phys. J. Exp. Theor. Phys+. 42, 279 (1975)
[44] O. Hemmers, W. Stolte, R. Guillemin, D. Rolles, D. Lindle, Bull. Am. Phys. Soc. 50, 40 (2005)
[45] A.B. Voitkiv, B.G. Krakov, Zh. Tech. Fiz. 68, 20 (1998)
[46] D.F. Register, S.T. Trajmar, S.K. Srivastava, Phys. Rev. A 21, 1134 (1980)
[47] M.A. Uman, Lighting (McGraw-Hill Book Company, New York – St. Louis – San Francisco – Toronto – London – Sydney, 1969)